Geophysical Exploration of a Historical Stamp Mill Dump for the Volume Estimation of Valuable Residues

Martin, Tina; Kuhn, Kerstin; Günther, Thomas; Knieß, Rudolf

Published in:
Journal of Environmental and Engineering Geophysics

DOI:
10.2113/JEEG19-080

2020

Document Version:
Publisher's PDF, also known as Version of record

Journal of Environmental and Engineering Geophysics

June 2020
Volume 25
Issue 2
pp. 275–286
DOI: #10.2113/JEEG19-080

Geophysical Exploration of a Historical Stamp Mill Dump for the Volume Estimation of Valuable Residues

Tina Martin[1,*], Kerstin Kuhn[1], Thomas Günther[2] and Rudolf Kniess[1,†]

[1]Federal Institute for Geosciences and Natural Resources (BGR) Stilleweg 2, D-30655 Hannover, Germany
[2]Leibniz Institute for Applied Geophysics (LIAG) Stilleweg 2, D-30655 Hannover, Germany

*Currrently residing at Lund University, John Ericssons väg 1, SE-22363 Lund, Sweden
†Currently residing at Eastern Atlas GmbH & Co.KG Berliner Str. 69, D-13189 Berlin, Germany

ABSTRACT

We present an approach for the estimation of ore processing residue volumes in historical mine waste dumps by the use of different geophysical methods in combination with mineralogical investigations. The stamp mill dump in the Harz mountains, Germany was examined with the methods electrical resistivity tomography (ERT), ground penetrating radar (GPR) and spectral induced polarization (SIP) flanked by mineralogical studies at many drilling points. The mineralogical results were used to calibrate the geophysical results and to distinguish between valuable and non-valuable waste material. With SIP we investigated individual profiles and took lab samples. These lab results emphasize the differences between the fine-grained tailings of clayey silt to silty sand in the top layer and the sandy tailings underneath in both resistivity and phase. From the GPR results we can distinguish between different layers and various backfillings in the first two meters due to the much higher resolution than the other methods. From ERT we achieved an overview about the dimension and inner structure of the dump and the boundary between the sandy residual material and the host rock. To estimate the volume of the residual body we carried out 2D inversion of all ERT profiles followed interpolation between the inverted profiles. From the drilling interpretation, the SIP lab results and the ERT field measurements we defined a resistivity threshold of 350 ohm-m for the ore processing residues to achieve a 3-dimensional body of the dump. The volume of this body was then corrected by a factor due to consideration of uncertainties, *e.g.*, forest areas, inaccessible dump sections, small-scale anomalies (geological or different anthropogenic nature) and inversion coverage. As a result, we were able to calculate the volume of the ore processing residues which can be used further for the determination of the economic potential (remaining metal content).

INTRODUCTION

Due to volatile commodity markets and the aim for an increasing circular economy, historic anthropogenic dumps are increasingly becoming exploration targets. A contribution to the supply of raw material are new research approaches for investigating historical mine waste dumps and providing predictions about the residual material. This material can still contain an appreciable amount of metals, which might be worthwhile to extract. For centuries mine waste dumps were applied to dispose waste rock, low grade ore, tailings, and metallurgical waste (*e.g.*, slags, flue ashes, dust). For example, the Harz mountains/Germany were rich in several metals including silver, lead, zinc, copper, and iron ore so the mining was an important economic sector and the landscape is embossed by historical mining relics and dumps. But due to the batch-wise deposition (especially of older residues), changes in the mined crude ore and the applied processing techniques, historical waste dumps are often very heterogeneous regarding mineral composition and dump structure. It is therefore necessary to detect the structures with suitable methods in order to determine areas for recycling in terms of size and location as well as the content of residues.

For such investigations geophysical methods, combined with geotechnical, geochemical, and mineralogical methods, can be used. One of the most common geophysical measurement techniques for investigating near-surface structures such as layering and the discrimination of the subsurface material, is the electrical resistivity tomography method (ERT) (*e.g.*, Benson *et al.*, 1983; Ward, 1988; Bernstone *et al.*, 2000; Campbell and Fitterman, 2000; Ullrich *et al.*, 2007a; Martinez-Pagan *et al.*, 2009). Due to the dump material, which is often characterized by different resistivities relative to the host material (Campbell and Fitterman, 2000), various subsurface can often be discriminated with ERT. An extension of this method is the induced polarization (IP) method which provides, in addition to the resistivity, information about the concentrations of disseminated ore minerals (*e.g.*, Pelton *et al.*, 1978; Seigel *et al.*, 1997; Ward, 1988; Hupfer *et al.*, 2016). It can also be applied for

Figure 1 (a) Location (source: wikimedia commons); and (b) drone view of the investigated historical Bergwerkswohlfahrt mine waste dump, Clausthal-Zellerfeld, Harz mountains, Germany.

quantification of slag heap volumes at historical slag sites for archaeological purposes (Florsch *et al.*, 2011, 2012, 2017) or for the prospection of new ore deposits in dumped slag heaps (Qi *et al.*, 2018) as well as for determining the exact limitation of slag heaps and differentiate the slags from soil (Weller *et al.*, 2000; Ullrich *et al.*, 2007b, c; Meyer *et al.*, 2007).

Furthermore, the ground penetrating radar (GPR) technique is a method for the investigation of very shallow parts of a dump/heap (Meyer *et al.*, 2007; Ullrich *et al.*, 2007b). Bergstr̆om (1998) showed that GPR is a powerful method for investigation of the structural integrity of a sealing layer in a mining waste dump. Near surface horizontal layers can be detected and tracked very well with GPR. But due to the mostly conductive material (Campbell and Fitterman, 2000; Benson *et al.*, 1983) the penetration depth of the radar waves is often weak, and only the upper subsurface can be usually measured. Combining and integrating different geophysical techniques can provide even more valuable information about the characterization and internal structure of mining dump, waste rock piles (Campos *et al.*, 2003; Anterrieu *et al.*, 2010; Power *et al.*, 2018) and tailings facilities (DeVos *et al.*, 1997; Van Dam *et al.*, 2005; Poisson *et al.*, 2009) than a single method.

The aim of this study was to determine the dimension and the inner structure of a historical mine waste dump in the Harz Mountains as well as the estimation of the volume of mine waste residues with high reprocessing potential. This was done by different geophysical methods in combination with the mineralogical results of drilling cores. We used the ERT method to assess the dimension of the dump. To discriminate between the different material and to assist the ERT measurements we used the spectral (S)IP technique. GPR was also applied in order to study and reconstruct the first few meters (1–2 m) of the subsurface with a very high resolution. For the interpretation of the geophysical results various drill cores were taken at different places within the investigated dump. The combined analysis of the results enabled an estimation of the valuable residual volume.

SITE DESCRIPTION AND HISTORY

The investigated *Bergwerkswohlfahrt* mine waste dump is situated in the central part of Germany in the Harz mountains (Fig. 1(a)) and was active from 1903 until 1931 (Mining Archive of Lower Saxony). At *Bergwerkswohlfahrt*, hydrothermal vein ore from the eastern part of the Silbernaaler vein system was mined for silver and lead. Water-powered stamp mills in combination with gravity separation were used in the beneficiation process. At the beginning of the 20th century (1903–1914), the capacity of the ore processing plant was about 25,000–30,000 tons of processed ore per year. Later on (from 1916), up to 40,500 tons per year of ore were mined in peak times (Bartels, 1992). The fine-grained fraction of the tailings from crushing and tabling still contained 3% lead. Starting from 1924 the slurries were additionally grinded below 0.1 mm and flotated, resulting in a separate lead concentrate with 50 to 60% lead (Bartels, 1992). Coarse-grained residues were still separated by traditional tabling procedures. The ore processing plant *Bergwerkswohlfahrt* was closed in 1931 and the mined ore was transported to the processing plant of the nearby *Hilfe Gottes* mine site. Nowadays, the closed *Bergwerkswohlfahrt* mine waste dump is about 400 m long, wedge-shaped and located next to the *Innerste* stream. The dump has quite a heterogeneous appearance with uncovered ore processing residues and vegetated areas covered by plants and trees (Fig. 1(b)). Small digs in the wooded areas up to half a meter depths revealed blocky rock material in combination with loam. Presumably, these are residues that were deposited during the subsequent use as a construction and mineral waste disposal site. As some of the steep slopes are still uncovered, an input of waste material into the adjacent stream takes place.

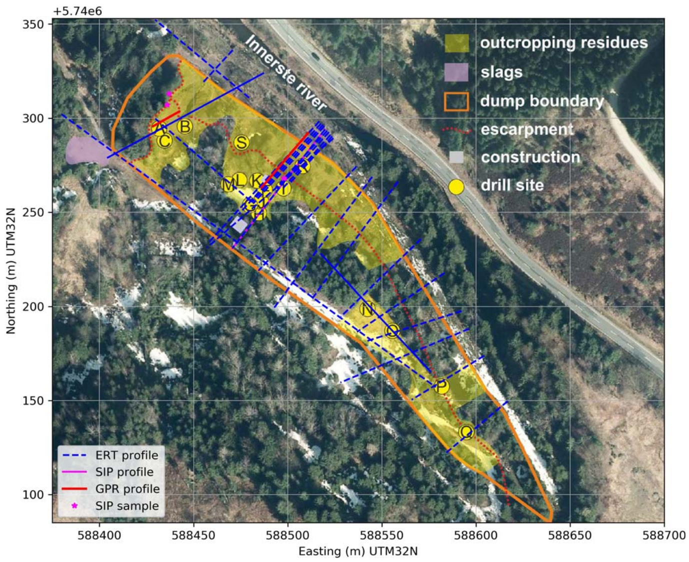

Figure 2 Overview of the locations of used ERT (blue), SIP (magenta) and GPR (red) profiles, SIP sampling positions (magenta stars) and drilling points (modified after Kuhn and Meima, 2019). Solid ERT lines are discussed in detail, dashed and solid ERT lines are used for volume estimation.

Therefore, remediation of the dump is needed and planned.

MATERIALS AND METHODS

Drilling

Based on the geophysical measurements, 16 drill cores were taken by direct push core drilling (Fig. 2, red squares). Due to the small diameter of the drill pipe (5 cm) and the included plastic liners, a sampling of the coarse-grained blocky material was not possible (Kuhn and Meima, 2019). The drill cores could be rammed down until 4 to 8 m depth and then mostly got stuck in the underlying blocky material. This underlying material consists of blocky host rock or hardly mineralized mining waste, which could contain lower amounts of gangue and ore minerals. These hardly mineralized mining waste usually derives from the construction of adits, shafts or surface infrastructure. For the following text we will only refer to host rock but always mean both the host rock and the hardly mineralized mining waste.

The ore processing waste (tailings) of the mine waste dump consists of different layers, which are distinguishable by their grain size. These layers are predominantly made up of sand, silty sand or clayey silt, but they also intermix (Kuhn and Meima, 2019). The residues are made of gangue minerals, ore minerals, and host rock fragments, which are partially intergrown. Compared to tailings from froth flotation, the residues from the gravity separation of *Bergwerkswohlfahrt* contain very high concentrations of lead, antimony, and silver. As the grain size decreases, the average base metal concentrations of lead, antimony and silver as well as the degree of weathering increase. Thus, the highest metal concentrations with median concentrations of 8.6 wt% occur in the clayey silt layers. Median metal concentrations of the ore processing waste of the mine waste dump are about 4.6 wt% Pb, 0.1 wt% Zn, 270 ppm Sb, 200 ppm Cu, and 110 ppm Ag. Valuable metals not only occur in the primary sulfides, but also in secondary phases, especially in cerussite ($PbCO_3$) and Fe oxyhydroxides (Kuhn and Meima, 2019).

In the northwestern area and in parts of the central area of the dump, the sandy tailings are covered by an approximately 1 m thick layer of clayey silt. The geochemical and mineralogical composition of this layer is similar to thin clayey silt layers occurring within the dump. The clayey silt layers could represent former slurries from the tabling process, which originally were deposited in basins and heaped up on *Bergwerkswohlfahrt* from time to time (Kuhn and Meima, 2019).

In Fig. 3, the alternating strata within the dump is exemplified for one drill core (G, refer to Kuhn and Meima (2019) for a detailed description). The first 2.7 m are made up of alternating sand, silty sand and clayey silt layers. Below 2.7 m the underlying blocky mining waste or host rock was sampled. Because direct push drilling does not allow for casing of the drill hole, caving material occurs in the drill cores. The caving material derives from loose material that fell into the drill hole during the time that the drill pipes were outside the hole to extend their length. The caving material was excluded from any analyses or interpretation.

Ground Penetrating Radar

Ground penetrating radar is a well-known geophysical method and often applied for example, the determination of buried structured like pipelines and cables, the detection of cavities or the investigation of near surface layers (*e.g.*, Butler, 2005; Kñodel *et al.*, 2007).

For our investigations we used the GSSI device SIR3000 with 200 MHz and 100 MHz antennas. Profiles were acquired using free positioning on a GNSS base-rover system from Novatel (DL V3) or an odometer. Particularly in the forested areas, free positioning was often not possible. The velocity model of the subsurface for the electromagnetic waves has been derived from well log data, so the depths of the reflectors could be determined. Each individual radargram was read and processed with the software ReflexW (Sandmeier, 2018) by a standard processing routine, which includes an offset correction, four times stacking, background removal, and resampling to 10 cm scanning distance. Manually set gain function depending on the travel time of the impulse were found to adjust an equally distributed amplitude level. The recording time per scan was adapted to the subsurface conditions and chosen in such a way that all usable signals were acquired. For profiles with free positioning, the parallel recorded GPS data over time were first linked with the radar. The scanning points between the individual GPS points were interpolated, so that each scanning point has a valid coordinate. From more than 50 profiles, we present in this study the results from two selected profiles at locations where drillings were conducted (Fig. 2, white lines). Both profiles have a length of 40 m (slope profile 23), resp. 16 m (profile 17) and were measured with the 200 MHz antenna.

Electrical Resistivity Tomography

The ERT method is also a very common and well known direct current (DC) or very low-frequency (2–8 Hz) alternating current (AC) resistivity technique and used for the investigation of lithological underground structure, the detection of soil inhomogeneities or the localization of aquifers (*e.g.*, Butler, 2005; Knödel *et al.*, 2007). Here, we measured 27 ERT profiles (Fig. 2) in three different field campaigns within 16 months, using the Wenner-alpha array. For comparison purpose some selected profiles were also measured with the Schlumberger and dipole-dipole arrays, but due to the similar results not shown here. The length of the profiles as well as the numbers of the used electrodes varied between 25 m (26 electrodes) and 99 m (100 electrodes). The electrode spacing was 1 m, only profile 5 had an electrode spacing of 2.5 m (covering a profile length of 247.5 m). For all measurements we used the Geotom instrument (*GeoLog*) with six channels and up to 100 electrodes. We used stainless steel electrodes with a coupling resistance of less than 10 kohms and current at a frequency of $f = 1.04$ Hz or 4.167 Hz. The data were analyzed two-dimensionally with the BERT algorithm (Günther *et al.*, 2006; Günther and Rücker, 2019) taking the topography into account. The mean relative root mean square (RMS) error for all profiles was around 4% (except profile 19 with 22%, probably due to bad electrode contact and therefore bad data quality).

Spectral Induced Polarization

The SIP method is an enhancement of an ERT measurement with AC. Besides resistivity, the phase displacement between the injected current and the measured potential signal is recorded. This displacement can provide information about capacitive effects in the underground and is often used for the detection of minerals, but also to address hydrological and environmental questions (*e.g.*, Kemna *et al.*, 2012). Analog to the ERT method, a 4-point electrode

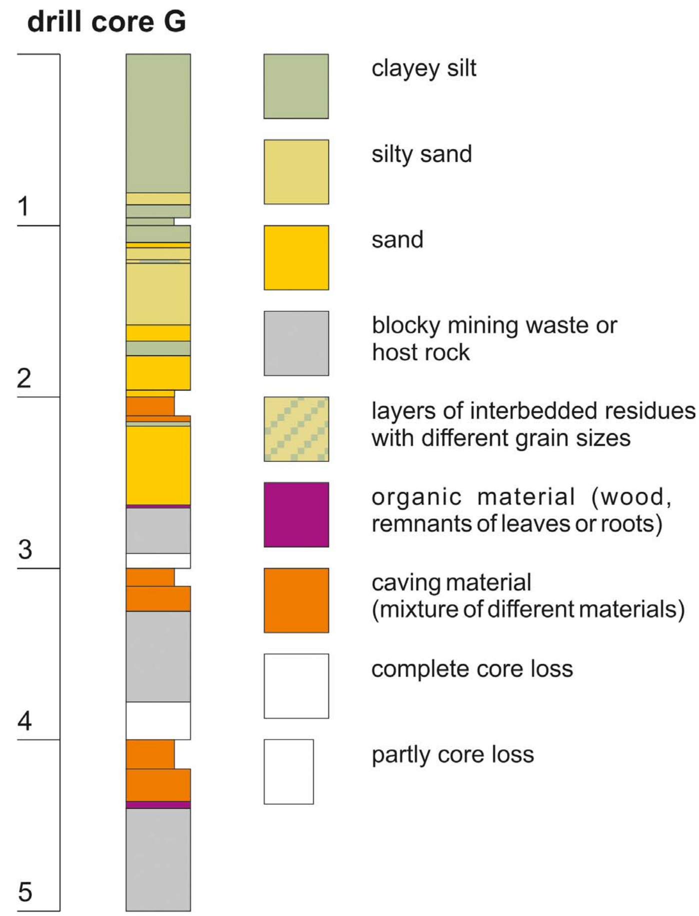

Figure 3 Lithology of one drill core (core G) showing the heterogeneity of the mine waste dump. Detailed analysis is available in Kuhn and Meima (2019).

configuration arrangement is required and conducted along a profile. Here, we used the device SIP 256C from Radic Research (Radic, 2004) with a varying number of remote units. The used electrodes were either unpolarizable (Ag-AgCl) to avoid polarization effects or separated stainless steel stakes for current injection and potential measurement. According to the investigations made by Zarif *et al.* (2017), the choice of the electrodes is mainly of second order. Even though, the main impact on IP measurements comes from the signal to noise ratio, we conducted dipole-dipole array but using only the forward potential dipoles to avoid unwanted phase shifts. Due to digitizing the signal directly at the potential dipole unit, the influence of the current-carrying cable can be minimized. The profiles were measured at 14 frequencies in a maximum frequency range between 0.07 Hz and 1000 Hz. We used the BERT algorithm (Günther *et al.*, 2006) for the inversion to generate frequency-dependent 2D depth sections of both parameters, resistivity and phase.

In addition to the field SIP measurements we also conducted SIP lab measurements. For the laboratory application the system SIP-ZEL from Forschungszentrum Jülich (Zimmermann *et al.*, 2008) with two

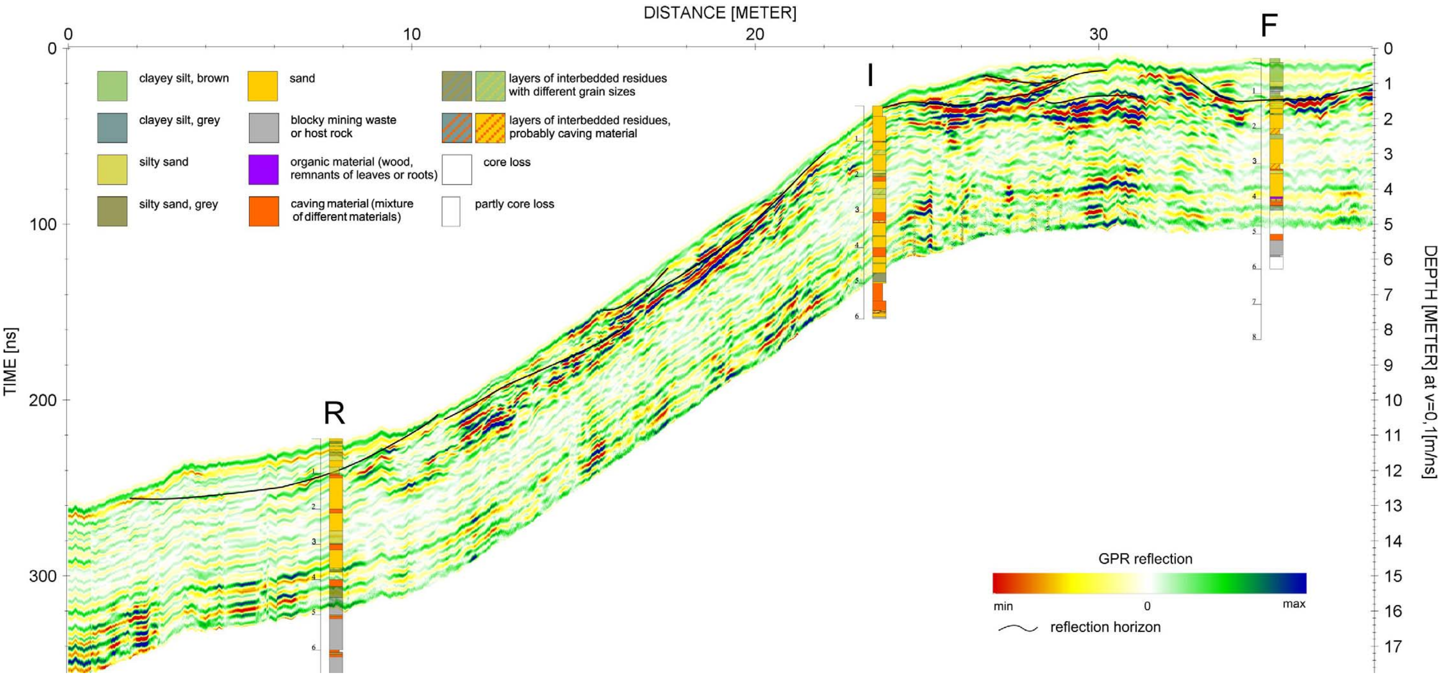

Figure 4 Results of GPR profile 23 collected with a 200 MHz GSSI antenna together with the drill core results. Below 2–3 m the GPR signals become weak and the radargram is mainly affected by antenna and device effects.

amplifiers for simultaneous measurements of two samples was used. The measurements took place in a climate chamber. For a detailed description of the laboratory measurement routine we refer to Hupfer *et al.* (2016).

At *Bergwerkswohlfahrt* six SIP profiles with different lengths were measured, using for five of the profiles the same electrodes and electrode distances as for ERT measurements. Instead, for SIP profile 6 we used unpolarizable electrodes. This profile was 44 m in length with an electrode spacing of 1 m and measured with a dipole-dipole configuration in a frequency range between 0.07 Hz and 1000 Hz. Additionally, we took samples from three different places and depths to investigate the material over a broader frequency range in lab (magenta stars in Fig. 2). Furthermore, at some selected samples mineralogical and chemical investigations were performed.

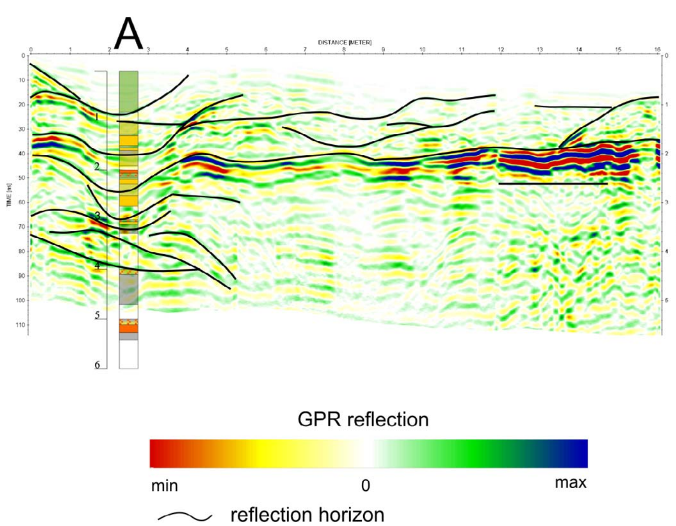

Figure 5 Results of GPR profile 17 (northern parts) with a 200 MHz GSSI antenna together with a drill core result. The legend of the drilling results can be found in Fig. 3.

RESULTS

Ground Penetrating Radar

In general, the results from the dump show many layer boundaries in the first 2 m (Fig. 4). On the plateau, numerous fillings/backfillings with dimensions of around 3-6 m can be observed. These small-scaled deposition structures were formed due to the batch-wise deposition of the tailings. In the slope areas, the deposition structures of the tailings are slightly different showing stronger layering. This probably originates from material sliding down the slope. Figs. 4 and 5 show representative GPR results for a slope profile (profile 23) and a plateau profile (profile 17, northern part of the dump), respectively, along with the results from the drilling. In the drill core results from the plateau (drilling F, Fig. 4) it can be seen, that the reflection horizon correlate very well with the boundary between the clayey silt and the sand material. At this drilling position, the blocky host rock starts at approx. 4 m depth, which can be hardly determined in the radargram due to the weak antenna signal. Below 2–3 m depth, antenna and device effects were mostly recorded.

At the plateau profile 17 (Fig. 5) various reflections can be noticed which are partly in accordance with

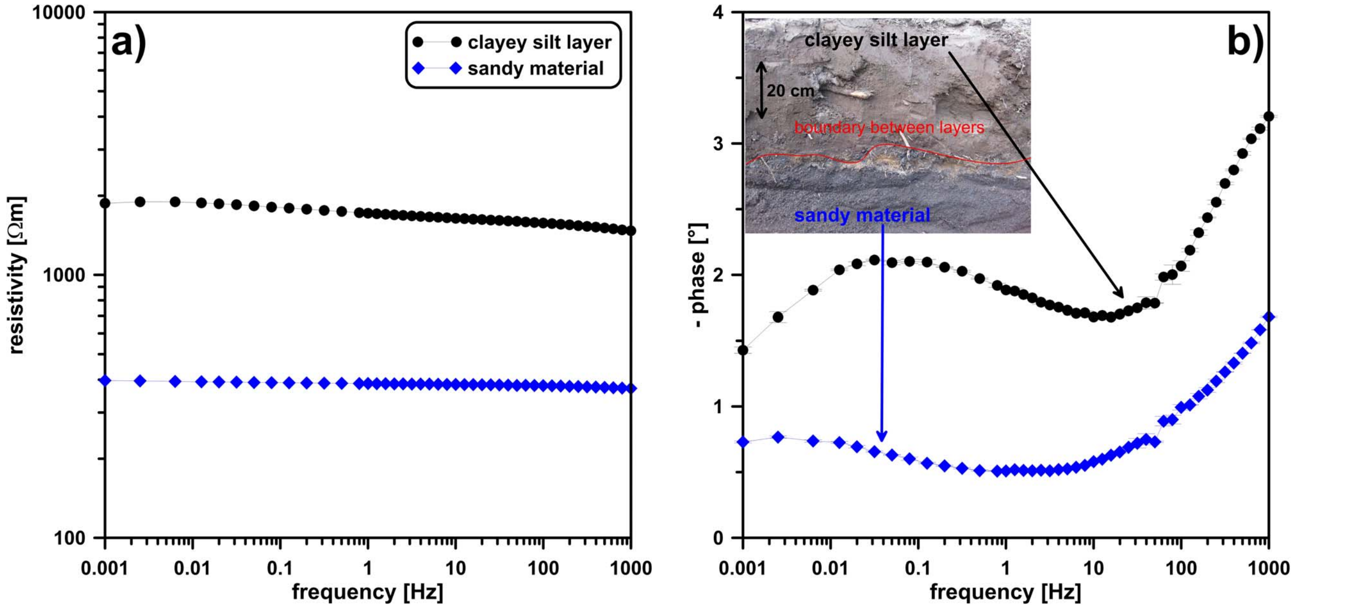

Figure 6 SIP lab results for the sandy (blue diamond) and the clayey silt material on the top (black dots): (a) resistivity; and (b) phase shift.

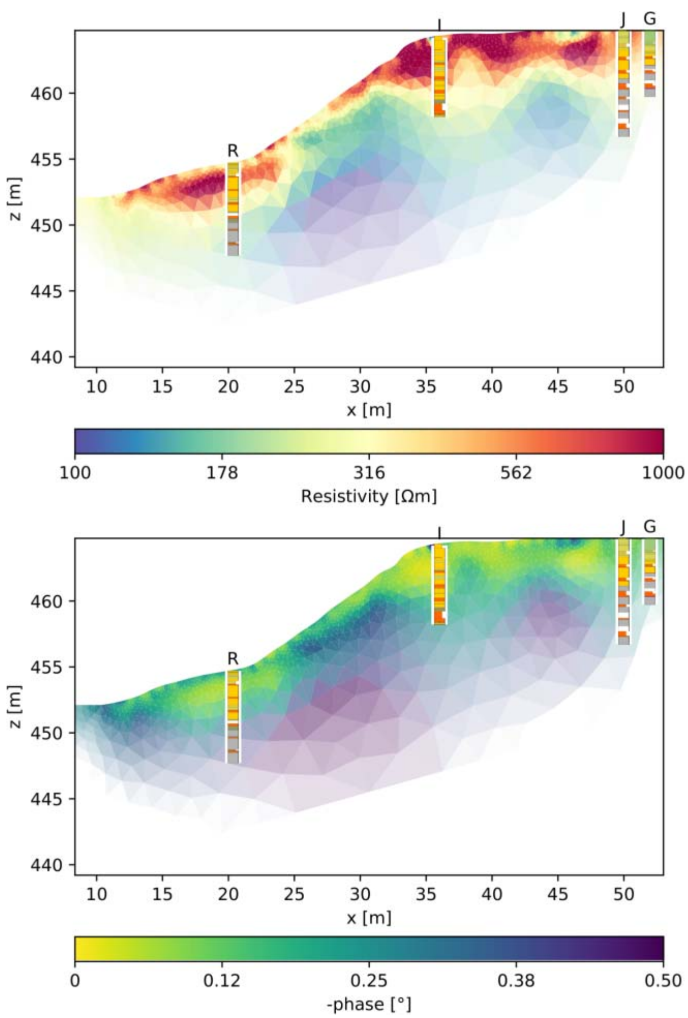

Figure 7 Inversion results for SIP profile 6 for a frequency f = 1.25 Hz. Resistivity is shown on top and phase shift is shown on bottom, together with the drill core data from the nearby cores R, I, J and G. The legend of the drilling results can be found in Fig. 3.

the variety of thin layers in the drilling results. The different layers mark the chronological order of the fillings over the active years of the mining dump. In the right part, a clear reflection horizon at about 2 m and some minor reflections are obvious, indicating a boundary between different filling materials. Also, the installation of building structures (*e.g.*, metal piles, reinforced concrete internals, etc.) can be seen.

Spectral Induced Polarization

The SIP results from the laboratory measurements show that the fine-grained clayey silt and silty sand materials, occurring in some regions of the dump in the upper 0.5–1 m surface layer, are characterized by high resistivities (up to 2000 ohm-m, Fig. 6(a)) and comparatively high phase effects (up to –2°, Fig. 6(b)). The underlying sandy material shows lower resistivities (≈400 ohm-m) and low phases (≈–0.5° at around f = 1.25 Hz).

In Fig. 7 the field inversion result from profile 6 are shown in resistivity (top) and phase (bottom) at frequency f = 1.25 Hz. A higher resistive layer (≥400 ohm-m, usually 3–4 m thick) can be seen which is thinning towards the escarpment (thickness approx. 2 m). In depth, the resistivity decreases down to 100 ohm-m. In phase, we observe a low polarizable (>–0.3°) top layer which correlates mainly with higher resistivities. In depth, the phase increases up to –0.7°.

Combining lab and field SIP results it is theoretically possible to distinguish three different materials (clayey silt/silty sand, sandy material, blocky host rock). However, in the field measurements the partly present 0.5–1 m thin clayey silt and silty sand layer identified with high resistivities (2000 ohm-m) and

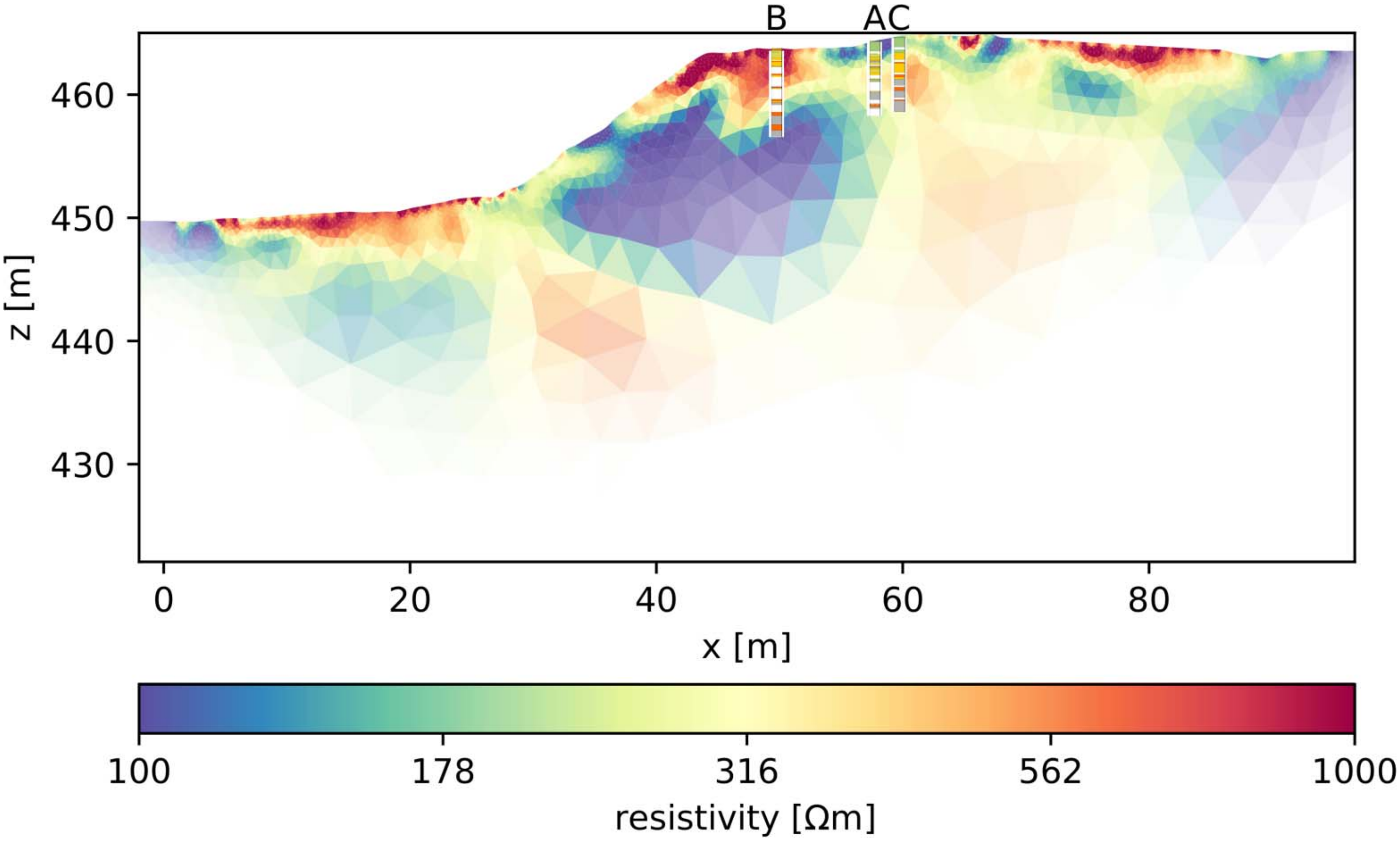

Figure 8 Resistivity inversion result of escarpment profile 4 along with the material distribution of three drillings (A, B, C) in the direct vicinity. The legend of the drilling results can be found in Fig. 3.

high phases (up to –2°) in the lab, can usually not be imaged/discriminated by SIP (or ERT). This is probably due to the electrode distance of >1 m, resulting in a lower resolution of the first meter. The underlying sandy material with very thin inter-bedded layers of silty sand or clayey silt is characterized by medium resistivities (400–1000 ohm-m) and low phases (>–0.3°). The laboratory results from the sandy material (approx. 400 ohm-m) correspond well with the inversion results from the field measurements. The wider range of resistivities probably results from the inter-bedded fine-grained layers.

The deepest layer is the blocky host rock material (resp. hardly mineralized mining waste) with low resistivities (≈100 ohm-m) and higher phases (up to –0.7°). Comparing these data with the drill core results (nearby cores R, I, J and G in Fig. 7) we observe a very good correlation between the sandy tailings and the underlying host rock.

Electrical Resistivity Tomography

From the ERT results it is obvious that the first visible layer is characterized by higher resistivities (red zones, >400 ohm-m) and the underlying host rock by lower resistivities (blue zones, <200 ohm-m). The resistive layer is less prominent on the escarpment than on the horizontal areas (Fig. 8). Out of the 27 ERT profiles (Fig. 2), the results of the escarpment profile 4 (Fig. 8) and the plateau profile 17 (Fig. 9) are exemplary discussed with neighbored drilling results (Fig. 2, straight blue lines). In general, the drilling results show a correlation between the sandy residual material and higher resistivities. The host rock is in accordance with lower resistivity areas.

The plateau profile (Fig. 9), located in the south-east part of the dump, is also characterized by a higher resistivity layer in the first meters whereas the underlying host rock (below 5 m) shows lower resistivities. Again, the drilling results from the boreholes N and P indicate higher resistivities for the sandy tailings. Interestingly, borehole O is located where the host rock gets close to the surface. The high resistivity zone between borehole N and O (in 10 m depth, at approx. profile meter 50 m) shows small-scaled anomaly. This anomaly might indicate different rocks with high resistivities or another anthropogenic filling, which is not necessarily ore processing material.

In Fig. 10, the 2D inversion results for all measured ERT (except profile 27 due to the high RMS error) profiles in *Bergwerkswohlfahrt* are illustrated in a 3-dimensional view. As in the shown ERT profiles and the SIP profile (Fig. 7(a)), the upper resistive layer (>400 ohm-m) can be found almost everywhere

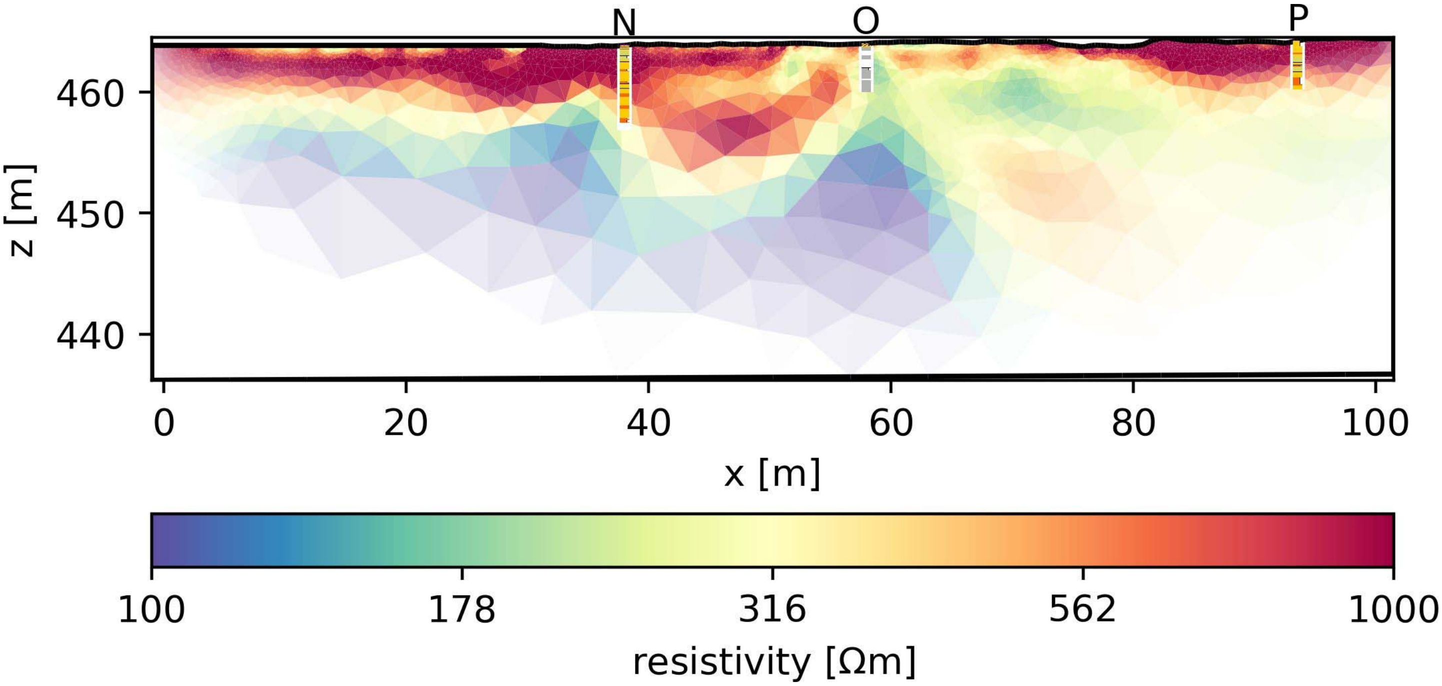

Figure 9 Resistivity inversion result of the plateau profile 17 along with the results from three close drillings N, O, P. The legend of the drilling results can be found in Fig. 3.

across the entire dump and reaches down to 5 m depth in some places. This zone is less prominent on the escarpment (to 2 m) and increases at the base of the escarpment edges again (Fig. 8). Below the high resistive layer, the resistivities decrease down to <200 ohm-m which correlates well with the occurrence of the blocky mine waste and host rock.

VOLUME ESTIMATION

To estimate the volume of the tailings within the mine waste dump different approaches were tried: Some parts of the profiles (profiles 6–14, central part of the dump) were inverted three-dimensionally due to the short distances between these profiles (max. 1.25 m) so a real 3D structure could be warranted. For this limited area of the stamp mill dump covered by these profiles, the inversion results were conclusive but it is not possible to draw conclusion about the entire dump area.

The second approach, conducting a 3D inversion using all ERT profiles was also not favorable due to the partially bad coverage in some parts of the dump (Fig. 10). Finally, after carrying out single 2D inversion for all profiles, we used interpolation of the inverted resistivity between them. To this end, we placed a triangular prism grid between the profiles (Fig. 11(a)). For each layer, the resistivity was interpolated horizontally independently to achieve a three-dimensional resistivity distribution.

From the SIP laboratory measurements it is known that both stamp mill samples have resistivities >400 ohm-m (Fig. 6). According to the ERT/SIP field results and the drill core analysis we achieved information about the resistivity boundary between the stamp mill material and the host rock, being in a range between 300 ohm-m and 400 ohm-m (Figs. 7–9). Therefore, we have chosen a threshold of 350 ohm-m, assuming that the material with lower resistivities are no stamp mill residues and therefore not valuable. After using this threshold, a volume body for the entire waste dump was calculated (Fig. 11(b)). The volume of this body is computed as $V_{2dInt} = 78{,}000\ m^3$.

The measured volume is affected by different uncertainties. Such uncertainties can be found, for example, in the wooded areas of the dump (Fig. 1). Much of the material in the forest areas has low resistivities, indicating a different material than the stamp mill residues. Therefore, most of the forest areas are already removed from the calculated model body (Fig. 11(b)). Nevertheless, smaller areas show higher resistivities, which might result from water uptake of trees. However, as these higher levels of resistivity only occur in some forest areas, we believe that in these areas stamp mill residues occur below the blocky material.

Furthermore, the ERT profiles (which were used for the volume body calculation) do not cover the entire area of the dump (especially in the south-west) due to rough and inaccessible terrain, so parts of the dump are not taken into account for the calculation (we estimated approximately 6–7%). In addition, particularly the regions close to the first or last ERT electrodes of each profile (start/end points) have lower/non data coverage and were therefore not fully

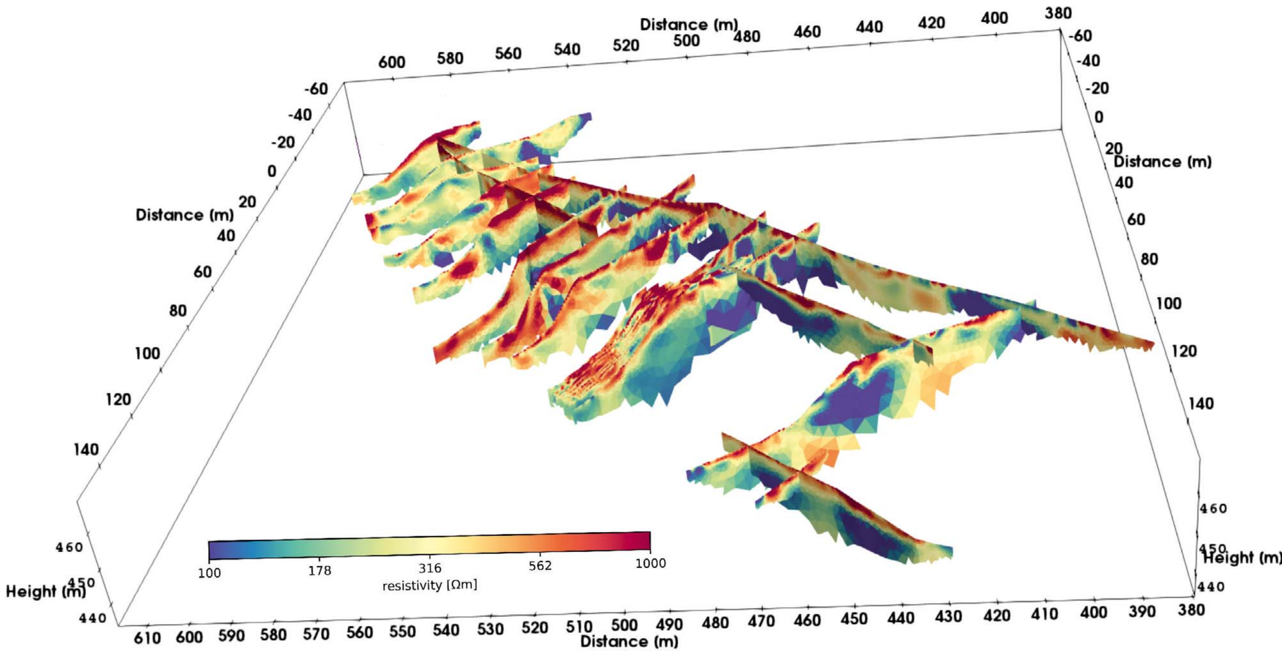

Figure 10 3-dimensional view of the 2D inversion results for all measured ERT profiles. The stamp mill waste areas are characterized by higher resistivities (red zones) and the host rock by lower resistivities (blue zones).

considered in the volume body determination. On the other hand, other small-scale anomalies can occur which might cause high resistive zones but should not be considered as stamp material (compare Fig. 9, near drilling O). Therefore, we assume a factor of 1–2% of the calculated volume which needs to be subtracted.

Considering both factors (the not covered terrains minus the small-scale high resistive anomalies), we end up in a correction factor of $Y_{corr} = 5\%$ which needs to be added to the above-mentioned volume body value:

$$V_{total} = V_{2dInt} + Y_{corr} \tag{1}$$

The final result is then computed to 81,900 m^3.

To determine a range of the possible volume, we calculated the volume body also with a threshold of 300 ohm-m as lower limit (103,000 m^3) and 400 ohm-m as upper limit (60,000 m^3). Correcting these results by the factor of 5% as well, we achieved values of 108,000 m^3 and 63,000 m^3. Resulting from these values we estimated the possible volume range with $\pm 25\%$.

DISCUSSION

The investigation of the inner structure of the dump and the calculation of the residual volume is based on the combination between three geophysical and a drilling technique. Each of the used methods was important to meet certain requirements.

With GPR we were able to distinguish between different fillings, which were formed due to the batch-wise deposition of the tailings. This is an important finding for the investigation of the metal distribution within the dump. It proves the occurrence of such fillings, which were hypothesized by Kuhn and Meima (2019). Areal variograms of the drill cores in the central area of the dump showed that the metal concentrations (*e.g.,* Pb) are spatially correlated only within a maximum range of up to 7–10 m, the assumed maximum extent of the fillings (Kuhn and Meima, 2019). The possibility of visualizing the occurrence of such fillings with GPR is important for estimating the error of the metal content calculation. As seen in the investigations of Kuhn and Meima (2019), the mineral content varies significantly with different layers. With GPR it is partly possible to distinguish between the uppermost clayey silt layer (which appears mainly in the northwestern area of the dump) and the sandy layers as long as the layer thickness is big enough (dm scale). Thin alternating layers of fine and coarser tailings could not be detected.

The advantage of the GPR method at a flat surface is the easy handling. However, on steep escarpments the realization of a good measurement is much more complicated. Furthermore, the investigation depth of the GPR is very limited due to strong attenuation (partly metallic dump installation), so at our site it was not possible to reach the lower layer boundary and to get a clear delineation between the residual material and the host rock. Furthermore, due to the partly strong topography 3D effects occur which also affect the radargram.

From the drillings we received mineralogical results and could therefore distinguish between the different stamp mill material (Kuhn and Meima, 2019).

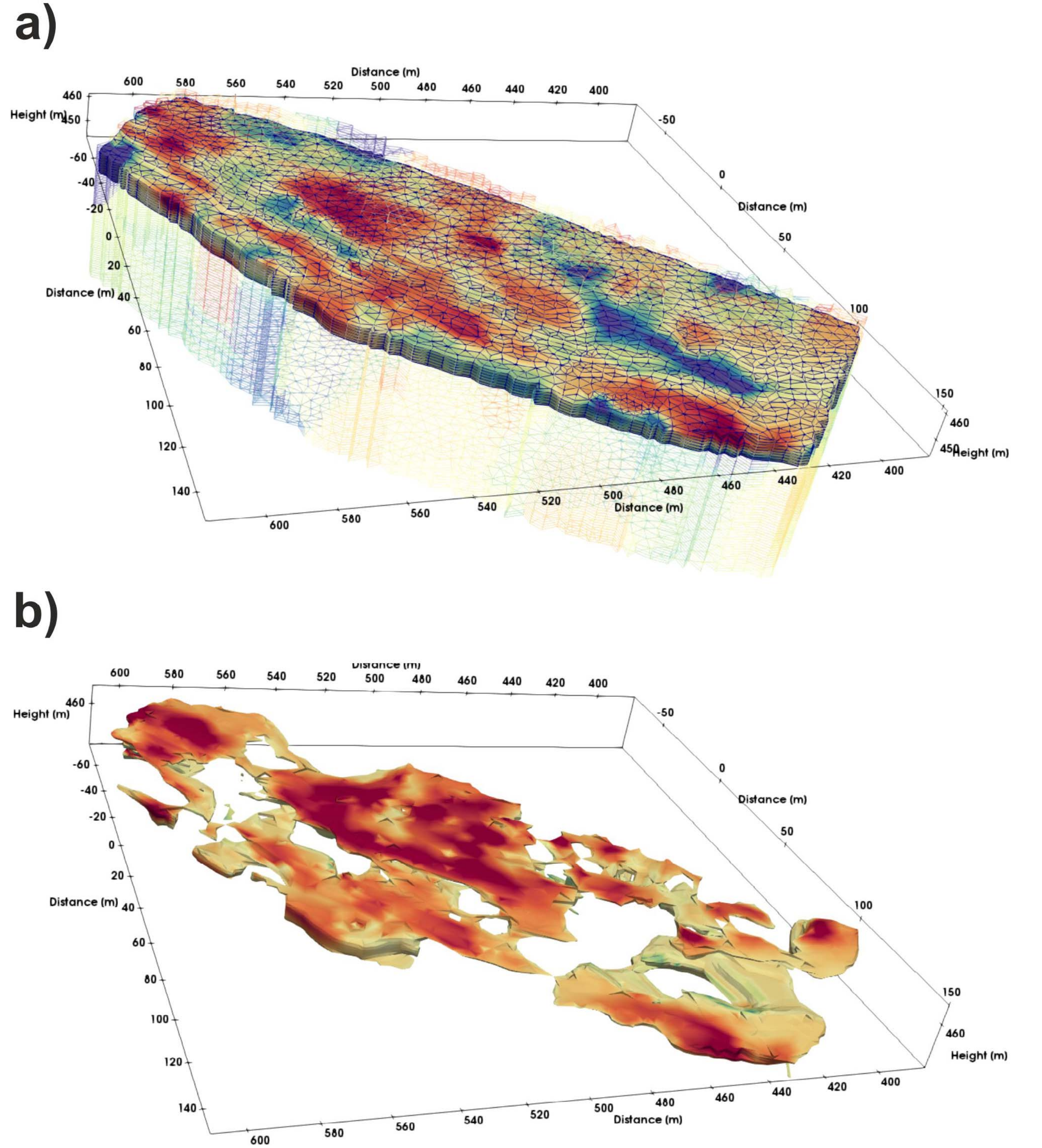

Figure 11 (a) Gridding mesh of the 3-dimensional interpolated resistivity results, which was used for the volume estimation; and (b) body of the estimated volume with a threshold of 350 ohm-m. The color scale can be found in Fig. 9.

Additionally, we correlate our GPR and ERT/SIP data with the mineralogical results, in order to be able to assign the electrical properties to different layers.

The results from the SIP measurements provided additional information. The data from the two different tailing samples which were investigated in the lab, have shown that the clayey tailings and the coarser tailings vary in their electrical behavior in both resistivity and phase. The phase signal was significantly higher for the clayey silt material than for the sandy material. From previous lab investigations (Hupfer *et al.*, 2016) and other literature (Pelton *et al.*, 1978; Campbell and Fitterman, 2000; Placencia-Gomez *et al.*, 2015) it is known that with increasing metal content the phase effect increases. According to Kuhn and Meima (2019) the highest metal content was found in the clayey silt layer, which is in accordance with our findings. Due to the low resolution in the first decimeters (due to the wide electrode spacing), the thin clayey silt layer occurring in the northwestern part of the dump on top, could not be seen clearly in the SIP field results. Compared to the clayey silt material, the sandy material from the lab investigation shows lower resistivities (400 ohm-m) and low phases. These values are more in accordance with the SIP field results (Fig. 7).

In general, the SIP method has the potential to characterize mining dumps or especially slag heaps (Weller *et al.*, 2000; Florsch *et al.*, 2011, 2012; Günther and Martin, 2016; Florsch *et al.*, 2017) much better than solely ERT measurements, in particular, when ore minerals are left in the residuals. At this field site, with the exception of the very shallow clayey material, we could not observe any higher phase effects from the residues in the measured field frequency range. Instead, we gathered higher phases from the host rock material than from the stronger mineralized tailings. But the contrast between the host rock and the tailings from ore processing are much higher in the resistivities than in the phase. Therefore, and due to the much longer acquisition time when measuring SIP in a broad frequency range (0.07–1,000 Hz) we acquired only a minor number of SIP profiles at this site.

Instead, most of the profiles were investigated with ERT. This method is easy to use and (relatively) fast, so several profiles could be measured per day. Depending on the length of the profile, we achieved good resolution until at least 10 m depth. Here, we could determine the lower boundary of the ore processing residues. However, the discrimination between the different residue layers (clayey silt, silty sand, sand) could not be resolved clearly due to the above-mentioned electrode distance ($\geq$1 m).

The approach for the volume estimation, presented in this study, is the result of the combination of different methods. We are aware that this calculation is just a rough estimation and influenced by many factors such as:

- ambiguity of the resistivity in inversion,
- resolution of the used geophysical and mineralogical methods,
- inaccessibility of the stamp mill waste in some areas,
- uncertainty from the interpolation,
- uncertainty by the estimation of forest areas and near-surface geological anomalies,
- saturation and temperature (which affects the resistivity).

Foremost, the first point shows the difficulties of a more reliable estimation. The small scaled anomaly between drilling N and O in Fig. 9 (at 55 m) is characterized by similar resistivities as the tailings. So, a distinction between both is hard to conduct (particularly in areas without drillings) and flows inadvertently into the calculation and may falsify the estimation, even when we tried to consider this by a correction factor (Y_{corr}). Naturally, there are further ways to improve the estimation. For example, to conduct more drillings, measure more ERT/SIP/GPR profiles, correct very small-scaled discrepancies by hand or take a-priori information from the drillings or GPR results (layer boundaries) into the ERT inversion. But most of them are time consuming and/or expensive and therefore not practicable.

Despite all difficulties and uncertainties, the estimation is the only way to obtain a volume of the valuable residues which provide a basis for metal content calculations and for the determination of the economic potential of the mine waste dump. Detailed geochemical and mineralogical investigation of the mine waste dump revealed that only Pb and Ag are of economic interest at *Bergwerkswohlfahrt* (Kuhn and Meima, 2019). These authors concluded that the dump is an interesting but limited secondary resource and the recycling might finance future remediation costs. The calculated amount of lead of 8000 t in the tailing is about 7.5% of the German netto imported lead from concentrates in 2018 (BGR, 2019).

CONCLUSIONS

The aim of this study was the estimation of valuable residuals and the detection of the inner structure of the stamp mill dump by using different geophysical and mineralogical techniques. The combination of the geophysical methods ERT, SIP and GPR along with the mineralogical drilling results enabled the determination of a potentially valuable material volume. Our approach to estimate the volume was based on the interpolation of all 2-dimensional inverted ERT profiles. Using the SIP, GPR and mineralogical results we defined a threshold for the ore processing residues. After the correction of different influences and uncertainties we obtained a value of approximately 82,000 m^3 ($\pm$25%).

To improve this estimation, more drillings or further ERT profiles can be conducted. Also, the extended use of the SIP method could give more valuable information to distinguish mineralogy, mineral content and grain size. Although it may not/never be possible to determine the exact volume of a historical dump, the techniques and approaches presented here have led to a convincing estimation of the amount of residues that can be used to determine the economic potential.

Even though, the combination of different methods has worked very well in our study, there is no universal method to estimate the volume of a mine waste dump. In fact, the methods, and the combination of them, needs to be carefully chosen and adapted to the specific requirements for each field site.

References

Anterrieu, O., Chouteau, M., and Aubertin, M., 2010, Geophysical characterization of the large-scale internal structure of a waste rock pile from a hard rock mine: Bulletin of Engineering Geology and the Environment, **69**, 533–548.

Bartels, C., 1992, Das Erzbergwerk Grund: Preussag AG Metall, Goslar.

Benson, R., Glaccum, R., and Noel, M., 1983, Geophysical techniques for sensing buried wastes and waste migration: National Ground Water Association, 236 p.

Bergström, J., 1998, Geophysical methods for investigating and monitoring the integrity of sealing layers on mining waste deposits: Licentiate thesis, Lulea University of Technology/Sweden, 77p.

Bernstone, C., Dahlin, T., Ohlsson, T., and Hogland, H., 2000, DC-resistivity mapping of internal landfill structures: Two pre-excavation surveys: Environmental Geology, **39**, 360–371.

BGR, 2019, Deutschland-Rohstoffsituation 2018, report, Federal Institute for Geosciences and Natural Resources, Hannover/Germany.

Butler, D.K., 2005, Near-Surface Geophysics: Society of Exploration Geophysicists.

Campbell, D.L. and Fitterman, D.V., 2000, Geoelectrical methods for investigating mine dumps, *in* Proceedings of the Fifth International Conference on Acid Rock Drainage. SME, 1513–1524.

Campos, D., Chouteau, M. Aubertin, M., and Bussi'ere, B., 2003, Using geophysical methods to image the internal structure of mine waste rock piles: Presented at the 9th EAGE/EEGS Meeting.

DeVos, K., Pehme, P., and Greenhouse, J., 1997, Ground geophysical surveys for mine wastes, *in* Proceedings of Exploration 1997, Fourth Decennial International Conference on Mineral Exploration, 917–926. (Toronto: Prospectors and Developers Association of Canada).

Florsch, N., Feras, A., Bonnenfant, J., and Camerlynck, C., 2017, La polarisation provoque, outil gophysique de spatialisation des amas de scories pour lestimation des productions sidrurgiques—induced polarization: A geophysical tool for slag characterization and ancient iron production assessment: ArcheoScience, **41-2**, 23–33.

Florsch, N., Llubes, M., and T'ereygeol, F., 2012, Induced polarization 3D tomography of an archaeological direct reduction slag heap: Near Surface Geophysics, **10**, 567–574.

Florsch, N., Llubes, M., T'ereygeol, F., Ghorbani, A., and Roblet, P., 2011, Quantification of slag heap volumes and masses through the use of induced polarization: Application to the Castel-Minier site: Journal of Archaeological Science, **38**, 438–451.

Günther, T., and Martin, T., 2016, Spectral two-dimensional inversion of frequency-domain induced polarization data from a mining slag heap: Journal of Applied Geophysics, **135**, 436–448.

Günther, T., and Rücker, C., 2009, Boundless Electrical Resistivity Tomography BERT—the user tutorial: 2.2 ed.

Günther, T., Rücker, C., and Spitzer, K., 2006, 3-d modeling and inversion of DC resistivity data incorporating topography—Part II: Inversion: Geophysical Journal International, **166**, 506–517.

Hupfer, S., Martin, T., Weller, A., Günther, T., Kuhn, K., Ngninjio, V.D.N., and Noell, U., 2016, Polarization effects of unconsolidated sulphide-sand-mixtures: Journal of Applied Geophysics, **135**, 456–465.

Kemna, A., Binley, A., Cassiani, G., Niederleithinger, E., Revil, A., Slater, L., Williams, K.H., Orozco, A., Haegel, F.-H., Hördt, A., Kruschwitz, S., Leroux, V., Titov, K., and Zimmermann, E., 2012, An overview of the spectral induced polarization method for near-surface applications: Near Surface Geophysics, **10**, 453–468.

Knödel, K., Lange, G., and Voigt, H.-J., 2007, Environmental Geology, BGR Bundesanstalt fuer Geowissenschaften und Rohstoffe ed.: Springer.

Kuhn, K., and Meima, J.A., 2019, Characterization and economic potential of historic tailings from gravity separation: Implications from a mine waste dump (Pb-Ag) in the Harz mountains mining district, Germany: Minerals, **9**, 303.

Martinez-Pagan, P., Cano, A.F., Aracil, E., and Arocena, J.M., 2009, Electrical resistivity imaging revealed the spatial properties of mine tailing ponds in the Sierra Minera of southeast Spain: Journal of Environmental and Engineering Geophysics, **14**, 63–76.

Meyer, C., Ullrich, B., and Barlieb, C.D., 2007, Archaeological questions and geophysical solutions: Ground penetrating radar and induced polarization investigations in Munigua, Spain: Archaeological Prospection, **14**, 202–212.

Pelton, W., Ward, S., Hallof, P., Sill, W., and Nelson, P., 1978, Mineral discrimination and removal of inductive coupling with multifrequency IP: Geophysics, **43**, 588–609.

Placencia-Gomez, E., Parviainen, A., Slater, L., and Leveinen, J., 2015, Spectral induced polarization (SIP) response of mine tailings: Journal of Contaminant Hydrology, **173**, 8–24.

Poisson, J., Chouteau, M., Aubertin, M., and Campos, D., 2009, Geophysical experiments to image the shallow internal structure and the moisture distribution of a mine waste rock pile: Journal of Applied Geophysics, **67**, 179–192.

Power, C., Tsourlos, P., Ramasamy, M., Nivorlis, A., and Mkandawire, M., 2018, Combined DC resistivity and induced polarization (DC-IP) for mapping the internal composition of a mine waste rock pile in Nova Scotia, Canada: Journal of Applied Geophysics, **150**, 40–51.

Qi, Y., Ahmed, A.S., Revil, A., Ghorbani, A., Abdulsamad, F., Florsch, N., and Bonnenfant, J., 2018, Induced polarization response of porous media with metallic particles part 7: Detection and quantification of buried slag heaps: Geophysics, **83**, E277–E291.

Radic, T., 2004, Manual SIP256C. Radic-Research, www.radic-research.de.

Sandmeier, K., 2018, Manual REFLEXW. Sandmeier geophysical research, www.sandmeier-geo.de.

Seigel, H.O., Vanhala, H., and Sheard, S.N., 1997, Some case histories of source discrimination using time domain spectral IP: Geophysics, **62**, 1394–1408.

Ullrich, B., Günther, T., and Rücker, C., 2007a, Electrical resistivity tomography methods for archaeological prospection, *in* Proceedings of the 35th International Conference on Computer Applications and Quantitative Methods in Archaeology (CAA).

Ullrich, B., Meyer, C., and Weller, A., 2007b, Geoelektrik und Georadar in der Archäologischen Forschung: Geophysikalische 3D-Untersuchungen in Munigua (Spanien), 76–93. Springer-Verlag Berlin Heidelberg.

Ullrich, B., Weller, A., Günther, T., and Rücker, C., 2007c, Geophysical prospecting of ancient slag deposits in Munigua (Spain) and Ain-al Hajer (Morocco) using complex resistivity tomography: Presented at the 2nd International Conference Archaeometallurgy in Europe, Aquileia/Italy.

Van Dam, R.L., Gutierrez, L.A., McLemore, V.T., Wilson, G.W., Hendrickx, J.M., and Walker, B.M., 2005, Near surface geophysics for the structural analysis of a mine rock pile, northern New Mexico: Presented at the National Meeting of the American Society of Mining and Reclamation, ASMR, 3134 Montavesta Rd., Lexington, KY 40502.

Ward, S.H., 1988, The resistivity and induced polarization methods, *in* Proceedings of the Symposium on the Application of Geophysics to Engineering and Environmental Problems, 109–250.

Weller, A., Brune, S., Hennig, T., and Kansy, A., 2000, Spectral induced polarization at a medieval smelting site: Presented at the 6th Meeting of Environmental and Engineering Geophysical Society (European Section).

Zarif, F., Kessouri, P., and Slater, L., 2017, Recommendations for field-scale induced polarization (IP) data acquisition and interpretation: Journal of Environmental and Engineering Geophysics, **22**, 395–410.

Zimmermann, E., Kemna, A., Berwix, J., Glaas, W., Münch, H., and Huisman, J., 2008, A high-accuracy impedance spectrometer for measuring sediments with low polarizability: Measurement Science and Technology, **19**, 105603.

Acknowledgments

We thank the German Ministry of Education and Research (BMBF) for funding the project ROBEHA (grant 033R105) in which all the work was done. Special thanks to Ursula Noell for the fruitful discussions and help with the manuscript. Furthermore, we acknowledge the help from our other colleagues Manfred Ratz, Ralf Seibold, Matthias Sack from BGR for their assistance during field work. We also acknowledge the comments and help from the reviewer Nicolas Florsch and the Associated Editor Remke van Dam, which improved our manuscript significantly.